Solution self-assembly of poly(3-hexylthiophene)-poly(lactide) brush copolymers: impact of side chain arrangement

Journal:	*Polymer Chemistry*
Manuscript ID	PY-ART-04-2018-000627.R1
Article Type:	Paper
Date Submitted by the Author:	16-May-2018

Complete List of Authors:	Ahn, Suk-kyun; Pusan National University, Polymer Science and Engineering NAM, JINWOO; Gwangju Institute of Science and Technology School of Materials Science and Engineering, School of Materials Science and Engineering Zhu, Jiahua; Oak Ridge National Laboratory, Center for Nanophase Materials Science Lee, Eunji; Gwangju Institute of Science and Technology, School of Materials Science and Engineering Kilbey, S.; University of Tennessee, Dept of Chemistry

SCHOLARONE™
Manuscripts

Please do not adjust margins

Journal Name

ARTICLE

Solution self-assembly of poly(3-hexylthiophene)-poly(lactide) brush copolymers: impact of side chain arrangement

Received 00th January 20xx,
Accepted 00th January 20xx

DOI: 10.1039/x0xx00000x

www.rsc.org/

Suk-kyun Ahn,*[a] Jinwoo Nam,[b,d] Jiahua Zhu,[c] Eunji Lee,*[d] and S. Michael Kilbey II[e]

We exploit the crowded intramolecular environment of brush copolymers and π-π interactions of poly(3-hexylthiophene) (P3HT) side chains to produce tailorable nanostructures by self-assembly in solution. A series of brush copolymers consisting of regioregular P3HT and amorphous poly(D,L-lactide) (PLA) side chains grafted on poly(norbornene) backbone are synthesized via ring-opening metathesis polymerization (ROMP) of norbornenyl-functionalized P3HT and PLA macromonomers. Three P3HT-PLA brush random copolymers and three brush block copolymers are prepared to create pairs of brush random and block copolymers containing comparable composition ratios of P3HT and PLA side chains. The relative volume fraction of P3HT and PLA side chains in the brush copolymers dictates thermal properties and crystallinity with little dependency on the side chain arrangement. However, the nanoscale morphologies of brush copolymers in a selective solvent are significantly altered by the side chain arrangement as well as copolymer composition. The different self-assembly behaviors in solution is attributed to the molecular design: In the brush block copolymers, self-assembly is driven by P3HT crystallization through both intra- and intermolecular π-π interactions, but intramolecular π-π interactions are largely suppressed in the brush random copolymers. Thus, tailoring brush copolymer architecture during synthesis enables additional levels of control over π-π interactions between P3HT side chains that are not present in conventional linear P3HT-based copolymers. The ability to use macromolecular chain topology as a way to access or tailor π-conjugated nanostructures may be beneficial in the context of controlling morphology at the nanoscale or producing patterned thin films for optoelectronic applications.

Introduction

The ability of block copolymers to spontaneously organize into a wide range of morphologies in solution has emerged as a promising approach to create of functional nanostructured materials with tunable physical and biological properties.[1, 2] When dispersed in a solvent selective for one block, block copolymers typically undergo microphase segregation and aggregation to generate nanostructures consisting of a core containing the insoluble blocks surrounded by corona comprised of the soluble blocks. Typical self-assembled nanoaggregates include spheres, cylinders, vesicles, and sheets, depending on molecular parameters such as relative block lengths, volume fraction, chain stiffness, and solubility of the blocks.[3-6]

The self-assembly of block copolymers consisting of π-conjugated core-forming blocks and semiconducting or insulating corona-forming blocks (i.e., rod-rod or rod-coil block copolymers) in a selective solvent provides improved control over self-assembled structures that can influence the performance of optoelectronic devices.[7-10] Among π-conjugated polymers, poly(3-alkylthiophene)-based (P3ATs) block copolymers have been extensively studied due to their potential in optoelectronic devices as well as facile synthetic preparation, which enables control of molecular weight, regioregularity, and chain functionality. In particular, the strong tendency of P3ATs to crystallize has been recognized as a major driving force for the efficient formation of π-conjugated aggregates.[11-16] A variety of nanostructures including nanowires,[17-19] spheres,[20-22] vesicles,[23] helical structures,[24] ribbons[25] and branched hierarchical structures[26, 27] have been created from P3AT-based block copolymers. Moreover, conductive and emissive nanowires are particularly appealing for their potential application as high performance organic semiconductors.[7] However, to-date most studies have focused on self-assembly of linear π-conjugated block copolymers.

The ability to tailor macromolecular chain topology is recognized as a powerful way to exert significant influence over properties and behaviors, including nanoscale organization, phase behavior, solubility and rheological properties.[28-31] In terms of π-conjugated macromolecules, altering the macromolecular chain topology can generate interesting self-assembled nanostructures that appear to be beneficial for organic electronics.[32-34] For

[a] Department of Polymer Science and Engineering, Pusan National University, Busan, 46241, Republic of Korea. Email: skahn@pusan.ac.kr
[b] Graduate School of Analytical Science and Technology, Chungnam National University, Daejeon 34134, Republic of Korea
[c] Center for Nanophase Materials Sciences, Oak Ridge National Laboratory, Oak Ridge, TN 37831, USA
[d] School of Materials Science and Engineering, Gwangju Institute of Science and Technology, Gwangju 61005, Republic of Korea. Email: eunjilee@gist.ac.kr
[e] Departments of Chemistry and Chemical and Biomolecular Engineering, University of Tennessee, Knoxville, TN 37996, USA
†Electronic Supplementary Information (ESI) available: See DOI: 10.1039/x0xx00000x

This journal is © The Royal Society of Chemistry 20xx

Please do not adjust margins

instance, Schenning et al. reported that star-shaped oligo(p-phenylenevinylene) self-assemble into a highly-ordered columnar superstructure in bulk, form π-stacked chiral fibers in solution, and organize into monolayers with a chiral hexagonal lattice arrangement at surfaces.[35] While polymeric materials generally suffer from high conformational entropy, enforcing conformational restrictions through topological constraints provides an attractive approach for organic electronic devices, which generally require structures with long-range order.

Bottlebrush polymers, also known as brush copolymers, are a class of architecturally complex polymers consisting of a long polymer backbone and densely-grafted, short polymer side chains.[36-40] The ability to widely tune the design of brush copolymers provides access to self-assembled nanostructures in melt,[41-43] thin film[44-46] and solution[47-49] that depart from structures adopted by simple linear copolymers. Beyond choices of monomer type(s) and molecular weight, the nonlinear chain topology offers a number of possibilities by which structure and properties of brush copolymers may be manipulated: the molecular weights of backbone and side chains,[50,51] grafting density,[43] composition,[52-54] arrangement of side chains,[55] and molecular symmetry[42,47] can be systematically adjusted during synthesis to affect nanoscale organization.

Here, we take advantage of the tunability of the brush copolymer architecture to produce tailored poly(3-hexylthiophene) (P3HT) self-assembled structures in solution. A series of brush copolymers consisting of π-conjugated regioregular P3HT and amorphous poly(D,L-lactide) (PLA) side chains were synthesized: amorphous PLA was chosen over crystalline poly(L-lactide) to avoid the formation of crystalline-crystalline brush copolymers and for their potential of faster degradation during hydrolysis. Specifically, three P3HT-PLA brush random (or mixed) copolymers and three brush block copolymers are prepared in such a way to generate pairs of brush random and block copolymers containing comparable compositional ratios of P3HT and PLA side chains. These pairs allow the impact of side chain arrangement and composition on the solution self-assembly of the P3HT-PLA brush copolymers to be investigated. The different brush copolymer designs allow π-π interactions between P3HT side chains to be regulated, which provides a useful way to vary the self-assembled nanostructure in a controlled manner.

Experimental

Materials

The fast-initiating ruthenium metathesis catalyst, $(H_2IMes)(pyr)_2(Cl)_2RuCHPh$, was synthesized as previously described[56] and quickly used after preparation. All other reagents were used as received unless otherwise noted.

Synthesis of macromonomers

The exo-norbornenyl-functionalized P3HT macromonomer (MM_{P3HT}) and exo-norbornenyl-functionalized PLA macromonomer (MM_{PLA}) were synthesized using procedures described in our previous publications.[57,58] In brief, MM_{P3HT} was made by a series of end-group functionalizations (Suzuki coupling followed by Steglich esterification) to transform the bromine end group of a P3HT to a norbonenyl end group, and MM_{PLA} was made by ring-opening polymerization of lactide by 5-norbornene-2-methanol. The number-average molecular weights of the macromonomers determined by end-group analysis using ^{1}H NMR spectroscopy, were 3.6 kDa for MM_{P3HT} (i.e., ~20 repeating units) and 5.3 kDa for MM_{PLA} (i.e., ~72 repeating units).

Synthesis of P3HT-PLA brush random and block copolymers

The synthesis of a P3HT-PLA brush random copolymer (see Scheme 1a) containing nearly equal amounts of MM_{P3HT} and MM_{PLA} is given as a representative example. The norbornenyl macromonomers, MM_{P3HT} (9.5 μmol) and MM_{PLA} (7.55 μmol), were added to an oven-dried 20 mL glass scintillation vial. The vial was then capped with a rubber septum. To this vial, 1.5 mL of dry chloroform were added via syringe and the headspace purged with nitrogen. In a separate vial, a stock solution (3.44 μmol, 0.344 mM) of $(H_2IMes)(pyr)_2(Cl)_2RuCHPh$ in dry chloroform (10 mL) was prepared and the headspace purged with nitrogen. Afterward, a portion of the catalyst solution (0.344 μmol, 1 mL) was transferred via syringe to the macromonomer solution. The mixture was stirred for 90 min at room temperature. To terminate the polymerization, an excess amount of ethyl vinyl ether (EVE, 0.1 mL) was added, and the mixture stirred for additional 5 min. The reaction mixture was concentrated, precipitated into methanol and filtered. The resulting precipitate was vacuum-dried overnight at room temperature.

P3HT-PLA brush block copolymers were synthesized by a similar procedure insofar as preparing solutions of monomer and catalyst; however, as shown in Scheme 1b, MM_{PLA} was first enchained and then MM_{P3HT} was added to the scintiallation vial. The isolation and purification of the brush block copolymers followed the same procedure that was used for the P3HT-PLA brush random copolymers.

Polymer characterization

^{1}H NMR spectra were acquired using a Varian Unity 500 wide bore multinuclear spectrometer with deuterated chloroform as solvent. Size exclusion chromatography (SEC) was performed using an Agilent 1260 Infinity binary pump equipped with Agilent 1200 Series PDA detector, a Wyatt Optilab T-rEX refractometer and a Wyatt Dawn Heleos II 18-angle laser light scattering detector. THF was used as eluent, and Wyatt ASTRA 6.1 software was used to calculate molecular weight and dispersity. Molecular weight of brush copolymers was determined by light scattering detection using specific refractive index increment of brush copolymers, $(dn/dc)_{copolymer}$, which was estimated based on a linear combination of the constituent macromonomers:

$$\left(\frac{dn}{dc}\right)_{copolymer} = w_{MM_{P3HT}}\left(\frac{dn}{dc}\right)_{MM_{P3HT}} + w_{MM_{PLA}}\left(\frac{dn}{dc}\right)_{MM_{PLA}}$$

where w_i and $(dn/dc)_i$ correspond to the mass fraction and refractive index increments of the macromonomers in the brush copolymer, and $(dn/dc)_i$ = 0.3 and 0.05 mL/g were used for MM_{P3HT} and MM_{PLA}, respectively, in THF.

This journal is © The Royal Society of Chemistry 20xx

Differential scanning calorimetry (DSC) measurements were performed using TA instruments (Q1000) with a heat/cool/heat protocol using an inert (nitrogen) atmosphere. Approximately 2-4 mg of a sample in a sealed platinum pan was heated to 250 °C to remove thermal history, then cooled to -100 °C, and re-heated to 250 °C. Each temperature ramp used a ramp rate of 10 °C/min. Thermal transition temperatures and associated enthalpy values were determined based on the first cooling and the second heating cycles. X-ray diffraction (XRD) measurements were performed on a Panalytical X'Pert Pro MPD equipped with an X'Celerator solid-state detector. X-rays were generated at 40 kV/50 mA and the beam wavelength was λ = 1.541 Å (Cu Kα radiation). For XRD measurements, films having thickness of ~250 µm were prepared by hot-pressing powder samples at 80 °C under a nitrogen environment using a Specac Mini-Film Maker. Absorption spectra were obtained using a UV-Vis spectrometer (NEOSYS-2000, Scinco, Seoul, Republic of Korea).

Transmission electron microscopy (TEM)

TEM images were obtained on a JEOL JEM-1400 (JEOL Ltd., Tokyo, Japan) operating at 120 kV, and the images were captured with a SC 1000 CCD camera (Gatan, Warrendale, PA, USA). The samples for TEM analyses were prepared by drop casting a 3 wt% of brush copolymer solution onto carbon-coated grids. The solvent used consisted of a mixture of THF and ethyl acetate (v/v = 60/40). THF is a common good solvent, while ethyl acetate is selective for PLA. We first dissolved the brush copolymers in THF and then slowly added ethyl acetate to the brush copolymer solution to induce aggregation. Images were analyzed using Simple Measure Program (JEOL Ltd., Tokyo) and Image J to determine the sizes of the self-assembled aggregates. To determine the diameter and length of self-assembled fibrils from TEM imaging, over 50 fibrils were analysed to generate the size distribution graphs (shown as Fig. S4†).

Results and discussion

Polymer synthesis

We synthesized a series of P3HT-PLA brush random and block copolymers using the same P3HT and PLA macromonomers (MM_{P3HT} and MM_{PLA}) but with varying composition. These brush copolymers were synthesized by ROMP using exo-norbornenyl-functionalized MM_{P3HT}, and exo-norbornenyl-functionalized MM_{PLA},

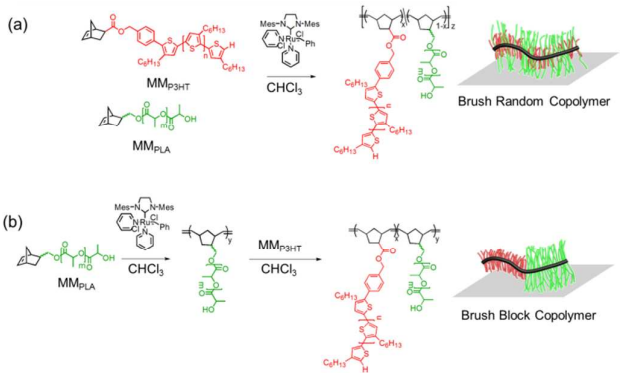

Scheme 1 Synthesis of P3HT-PLA brush copolymers: (a) brush random copolymer and (b) brush block copolymer.

as shown in Scheme 1. To produce the brush random copolymers, MM_{P3HT} and MM_{PLA} were simultaneously polymerized, while the brush block copolymers were obtained by sequential addition of MM_{PLA} and MM_{P3HT} during ROMP. The MM_{P3HT} and MM_{PLA} were synthesized separately using procedures described in our previous publications,[57,58] and their number-average molecular weights (M_n) determined by ^{1}H NMR analyses were 3.6 kDa (i.e., ~20 repeating units) for MM_{P3HT} and 5.3 kDa (i.e., ~72 repeating units) for MM_{PLA}.

The composition of brush copolymers was altered by adjusting the feed ratio of MM_{P3HT} and MM_{PLA}. Two sets of brush copolymers – pairs of random and block copolymers with three different compositions – were prepared. The composition of each pair of brush copolymers is comparable, as determined by ^{1}H NMR analysis based on the integrated ratio of peaks at 6.9 ppm (corresponding to proton at 4 position on thienyl rings of P3HT) and at 5.2 ppm (proton on backbone of repeating units of PLA) (Fig. S1†). Also, and as shown in Table 1, the theoretical molecular weight and the molecular weight measured by SEC (prior to purification) using multiangle laser light scattering (SEC-MALLS) of the brush copolymers are both ~220 kDa. Because these pairs of brush copolymers have comparable compositions and molecular weights, they allow the impact of side chain arrangement on the thermal properties, crystallinity and self-assembled structures in solution to be investigated. Throughout this article we refer to the brush random and block copolymers using Rx_{P3HT} and Bx_{P3HT} respectively, in which R stands for random and B stands for block, and *x* designates the composition, which is expressed as the volume % of P3HT side chain.

Table 1 Characteristics of P3HT-PLA brush random and block copolymers

Polymer	Vol_{P3HT}[a] (%)	Vol_{PLA}[b] (%)	Theo. M_n[b] (kDa)	M_w[c] (kDa)	$Đ$[c]	M_w[d] (kDa)	$Đ$[d]	Conv.[e] (%)
$R21_{P3HT}$	21	79	219	199	1.06	247	1.16	94
$R46_{P3HT}$	46	54	216	-	-	491	1.61	95
$R71_{P3HT}$	71	29	224	218	1.09	1323	1.72	93
$B23_{P3HT}$	23	77	219	219	1.06	289	1.27	96
$B49_{P3HT}$	49	51	219	-	-	355	1.31	93
$B70_{P3HT}$	70	30	225	241	1.12	750	1.64	96

[a]Determined by ^{1}H NMR assuming densities of 1.14 g/cm^3 for P3HT and 1.25 g/cm^3 for PLA, respectively. [b]Calculated as M_n = {[MM_{P3HT}]/[I] × M_n of MM_{P3HT}} +{[MM_{PLA}]/[I] × M_n of MM_{PLA}}. [c]Determined by light scattering detector from crude polymer solution before vacuum drying. [d]Determined by light scattering detector from polymer solution after vacuum drying. [e]Conversion is calculated using RI detector by comparing the peak area of brush copolymers to the peak area of residual macromonomers.

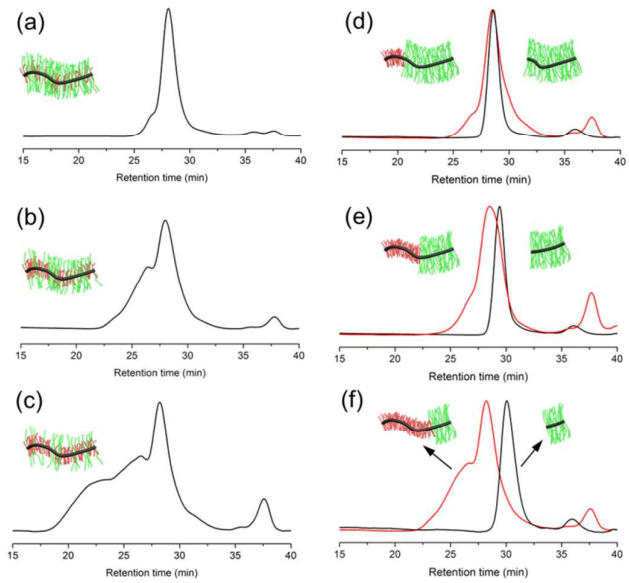

Fig. 1 SEC traces collected from RI detector of brush random and block copolymers after vacuum drying: (a) $R21_{P3HT}$, (b) $R46_{P3HT}$, (c) $R71_{P3HT}$, (d) $B23_{P3HT}$, (e) $B49_{P3HT}$, and (f) $B70_{P3HT}$.

Previously, we observed unusual, strong aggregation behavior from bottlebrush polymers having P3HT side chains. This aggregation, which was driven by attractive π-π interactions, was particular to brush architectures.[54,57] These aggregates were not apparent when the polymer was isolated by filtration from the crude reaction mixture, but appeared after freeze- or vacuum-drying processes. As a result, broad molecular weight distribution of products were seen in SEC traces and multiple distributions were observed by dynamic light scattering (DLS).[57] As seen in Fig. 1, a considerable amount of aggregation is also detected in both brush random and block copolymers, as evidenced by a broadening of the molecular weight distribution in SEC traces, especially at shorter retention time, which is indicative of chains of high molecular weight. The amount of aggregates is dependent on the composition of the brush copolymers. In general, higher P3HT composition leads to a stronger aggregation and aggregates of larger sizes, as reflected by the prominence of features in the SEC traces at shorter retention time. We note that black and red traces in Fig 1d, 1e and 1f represent PLA brush homopolymers and the chain extended P3HT-PLA brush block copolymers, respectively, and peaks at 35-38 min are due to unreacted MM_{P3HT} or MM_{PLA}. Included in the results of molecular characterization of the brush copolymers presented in Table 1 are molecular weights of the aggregates determined by SEC-MALLS, which shows that size of the aggregates increases as relative amount of P3HT increases in both brush random and block copolymers.

Thermal properties and crystallinity

The crystallization of regioregular P3HT-containing copolymers is driven by long-range interchain π-π stacking, which results in crystalline lamellae.[59-61] The P3HT-PLA brush random and block copolymers exhibit distinct melting and crystallization temperatures

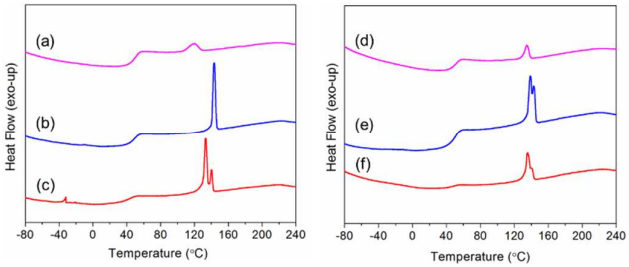

Fig. 2 DSC traces of P3HT-PLA brush random and block copolymers during first cooling: (a) $R21_{P3HT}$, (b) $R46_{P3HT}$, (c) $R71_{P3HT}$, (d) $B23_{P3HT}$, (e) $B49_{P3HT}$ and (f) $B70_{P3HT}$.

Table 2. Thermal properties of P3HT-PLA brush copolymers

Entry	T_g (°C)[a]	T_c (°C), [ΔH_c (J/g)][b]	T_m (°C), [ΔH_m (J/g)][a]
$R21_{P3HT}$	54.0	120.0, [2.5]	156.6, [2.6]
$R46_{P3HT}$	53.7	143.2, [6.8]	165.9, [5.8]
$R71_{P3HT}$	48.1	133.2, 140.1 [7.2]	159.5, [6.6]
$B23_{P3HT}$	56.1	134.6, [2.4]	168.1, [2.2]
$B49_{P3HT}$	55.3	138.7, 142.8, [5.1]	166.8, [4.4]
$B70_{P3HT}$	54.0	135.3, [6.6]	163.6, [7.4]

[a]Determined from the second heating cycle (Fig. S2†). [b]Determined from the first cooling cycle.

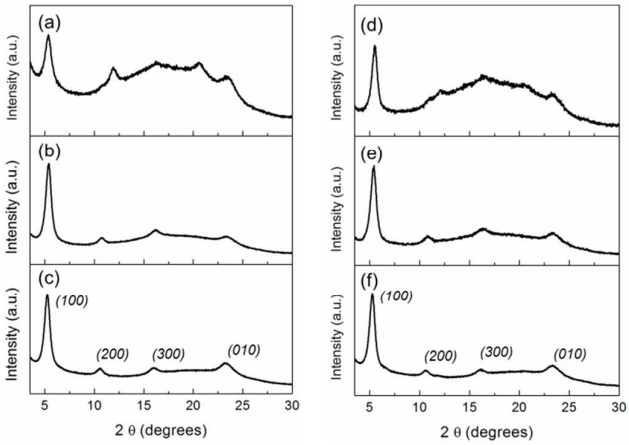

Fig. 3 X-ray diffractograms of P3HT-PLA brush random and block copolymers indicate lamellar microstructures and crystallization of P3HT across all copolymer compositions: (a) $R21_{P3HT}$, (b) $R46_{P3HT}$, (c) $R71_{P3HT}$, (d) $B23_{P3HT}$, (e) $B49_{P3HT}$, and (f) $B70_{P3HT}$.

(T_m and T_c) as shown in DSC thermograms (See Fig. 2 and Fig. S2†). Thermal transition temperatures and associated enthalpy values (ΔH_i) are summarized in Table 2. The brush random and block copolymers exhibit a glass transition temperature (T_g) associated with the PLA side chains and a T_c and T_m resulting from crystallinity of the P3HT side chains. Although a T_g of ~12 °C has been reported for P3HTs,[62] glass transitions corresponding to P3HT side chains are not clearly detected in either brush random or brush block copolymers.

Melting and crystallization temperatures and the corresponding enthalpies of the brush copolymers are highly dependent on the P3HT composition, as expected. In general, increasing the composition of P3HT side chain leads to an increase in T_m and T_c as well as the values of associated enthalpy. Interestingly, the compositionally symmetric brush random and block copolymers ($R46_{P3HT}$ and $B49_{P3HT}$) show T_m and T_c that are a few degrees higher than the P3HT-rich brush copolymers ($R71_{P3HT}$ and $B70_{P3HT}$). These

behaviors probably reflect differences in confined environments, which affect crystallization of the P3HT blocks. Similar behavior has been reported for other brush copolymers containing semicrystalline polymers as side chains.[63-66]

All of the brush random and block copolymers show XRD peaks characteristic of P3HT crystalline lamellae. As shown in Fig. 3, peaks assigned to (100), (200), and (300) corresponding to interlamellar distances in P3HT crystallites of ~1.6 nm are seen along with a (010) peak associated with the interchain π-π stacking distance of ~3.8 Å.[67] As the PLA content in the brush copolymers increases, the intensity of crystalline peaks gradually decreases while amorphous scattering becomes more pronounced. These results are in good agreement with observations derived from DSC studies which show a decrease in the enthalpy of crystallization, ΔH_c, with increasing PLA content. Thus, the relative composition of P3HT and PLA macromonomers is a key parameter that determines thermal properties and crystallinity of the brush copolymers in the melt state, regardless of the side chain arrangement.

Self-assembly behavior in solution

The strong π-π interactions between P3HT-containing polymers often result in the formation of well-defined, crystalline nanofibrils in the solution state. We hypothesize that the π-π interactions would be mediated by the side chain arrangement in the P3HT-PLA brush copolymers. To verify this, the morphologies adopted by the brush random and block copolymers when self-assembled in solution are examined by TEM. For these TEM studies, polymer solutions at a concentration of 0.3 mg/mL in a mixture of THF and ethyl acetate (v/v = 60/40) were drop-cast onto carbon-coated grids. This solvent mixture was used because THF is a common solvent for both P3HT and PLA side chains, but ethyl acetate is selective for PLA side chains. Therefore, the addition of ethyl acetate drives aggregation of P3HT side chains, and the solution color changes from orange to dark purple.

The representative TEM images shown in Fig. 4 and Fig. S3† clearly demonstrate that the side chain arrangement and composition have a dramatic impact on solution self-assembly of the brush copolymers. As observed from Fig. 4a and 4b, self-assembly of brush block copolymers $B49_{P3HT}$ and $B23_{P3HT}$ results in stiff, rod-like nanofibrils, with those formed from $B23_{P3HT}$ having a shorter length. The nanofibrils formed from $B49_{P3HT}$ and $B23_{P3HT}$ have similar diameters of 6.7±1.2 nm but different lengths, 89.9±18.0 nm and 50.8±13.9 nm, respectively (See Fig. S4†). The shorter length of $B23_{P3HT}$ nanofibrils compared to $B49_{P3HT}$ is probably due to the higher PLA content in $B23_{P3HT}$ mediating the attractive interactions between P3HT blocks that drives self-assembly of brush copolymers. Interestingly, markedly different morphologies are observed when the brush random copolymers are allowed to self-assemble in the mixed solvent. The brush random copolymer with intermediate P3HT content ($R46_{P3HT}$) shows a strong tendency to form flexible nanofibrils. These nanofibrils have a diameter of 6.1±1.1 nm and a length of 70.2±14.0 nm, as shown in Fig. 4c (and Fig. S4†). In addition and as seen from Fig. 4d, the brush random copolymer with the lowest P3HT content, $R21_{P3HT}$, adopts a nearly spherical aggregate structure with a diameter of 4.9±0.8 nm

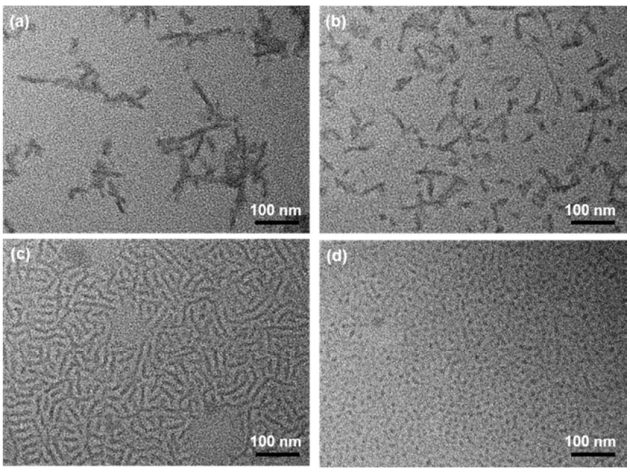

Fig. 4 TEM images of P3HT-PLA brush block and random copolymers created by drop-casting from a THF/ethyl acetate solvent mixture (v/v = 60/40). Linear fibrillar aggregates are observed for (a) $B49_{P3HT}$ and (b) $B23_{P3HT}$, while (c) $R46_{P3HT}$ forms non-persistent fibrillar aggregates and (d) $R21_{P3HT}$ adopts a spherical structure.

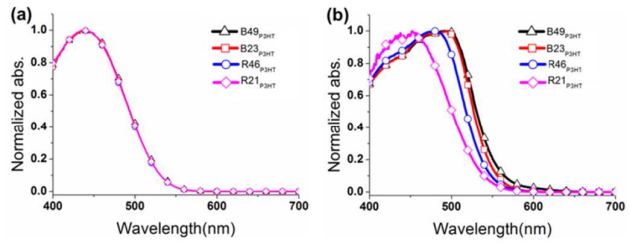

Fig. 5 UV-Vis absorption spectra of P3HT-PLA brush random and block copolymers in solution. Absorption spectra of brush copolymer solutions dissolved in (a) the good solvent THF overlay one another, exhibiting only a π-π* transition, while absorption spectra of self-assembled aggregates of brush copolymer solutions dissolved in (b) a THF/ethyl acetate mixture (v/v = 60/40) are red shifted due to aggregation brought by π-π stacking of P3HT side chains.

(Fig. S4†). The origin of the different morphologies created by self-assembly of brush random and block copolymers in solution will be discussed later. We note that the brush copolymers with high P3HT content, $R71_{P3HT}$ and $B70_{P3HT}$, had poor solubility in the THF/ethyl acetate mixed solvent and, as a result, their aggregates could not be analyzed by TEM.

Because of the color change (orange to purple) observed when ethyl acetate was added, UV-Vis spectroscopy was used to measure the optical absorbance of the brush copolymer solutions before and after the addition of ethyl acetate. As seen in Fig. 5, all of the brush copolymer solutions in the non-selective good solvent THF show only a single peak with an absorption maximum (λ_{max} = 440 nm), which is associated with the π-π* transition of fully dissolved P3HT chains and indicates no molecular ordering.[68] However, upon the addition of 40% ethyl acetate, the absorption peak maxima shift to longer wavelength, and λ_{max} appears to depend on topology and composition of the brush copolymers: 450 < λ_{max} < 495 nm. The changes in the absorption spectra are attributed to increases in the extent of aggregation, which is driven by intrachain and interchain π-π stacking of P3HT chains. In particular, the red shift in the absorption spectrum of the brush block copolymers was observed to be greater than that of the brush random copolymers. This suggests that there is an increase in the level of aggregation in

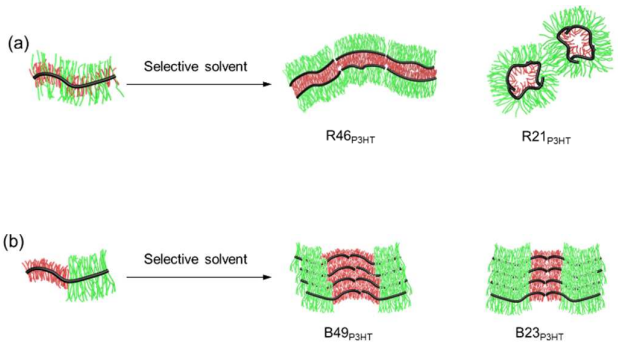

Fig. 6 Proposed self-assembly process of P3HT-PLA brush copolymers in solution with respect to the side chain arrangement and the composition: (a) P3HT-PLA brush random copolymer and (b) P3HT-PLA brush block copolymers. In each drawing, the thick black line represents the backbone, and green and red lines correspond to PLA side chains and P3HT side chains, respectively.

these samples. The shifts in λ_{max} are generally consistent with the changes in characteristic length of aggregates determined from TEM imaging. Also, we note that vibronic shoulders typically associated with interactions between organized, π-stacked P3HTs are absent from the absorption spectra, which suggests conformationally disordered structures are formed upon solution assembly of these brush copolymers.[69]

Importance of side chain arrangement for the solution self-assembly

The different morphologies resulting from solution self-assembly that are observed by TEM ostensibly originate from a strong dependence on side chain arrangement of the P3HT-PLA brush copolymers. When the poor solvent ethyl acetate is introduced, the P3HT side chains in the brush block copolymers associate by both inter- and intrachain π-π interactions. In this case, the conventional rigid nanofibrillar structures are favored regardless of the P3HT composition. By contrast, in the brush random copolymers, the intrachain interactions of P3HT side chains are highly disturbed by the presence of long PLA side chains. Therefore, interchain π-π interactions between P3HT side chains are major driving force for self-assembly, although their interactions become weaker in random arrangements compared to those of brush block copolymers. This inference is supported by the smaller red-shift in the UV-Vis absorption for random topologies, which suggests weaker π-π interactions. Additionally, composition seems to significantly influence the interfaces between P3HT and PLA domains in the brush random copolymers. Specifically, the brush random copolymer with symmetric composition ($R46_{P3HT}$) generates non-persistent nanofibrils, which suggests the formation of nearly flat interfaces. However, a higher PLA composition in the brush random copolymers ($R21_{P3HT}$) induces a larger interfacial curvature with a reduction of the interchain interaction between P3HT side chains, which generates the spherical morphology. The proposed self-assembly process of P3HT-PLA brush copolymers with respect to their side chain arrangement and composition are illustrated in Fig. 6.

Conclusions

We synthesized two sets of P3HT-PLA brush copolymers, random and diblock topologies, while holding total molecular weight fixed but varying composition. Through thermal measurements it is shown that in the melt state, the relative composition of the brush copolymers dictates thermal properties and overall crystallinity regardless of the side chain arrangement. However, brush random and block copolymers form different self-assembled structures in a selective solvent that are differentiated based on their side chain arrangement as well as copolymer composition. Solution self-assembly in a mixed solvent selective for PLA leads to the formation of non-persistent nanofibrils and spheres for brush random copolymer, but the brush block copolymers form highly persistent nanofibrils. While the design space of brush copolymers is vast, depending on side chain lengths, relative sizes, composition, and degree of polymerization, the ability to manipulate structures adopted by π-conjugated copolymers via chain topology (i.e., brush architecture) provides a useful strategy for creating well-ordered assemblies of π-conjugated polymers, which may aid the development of high performance organic semiconductors or thin film assemblies for optoelectronic devices.

Conflicts of interest

There are no conflicts to declare.

Acknowledgements

A portion of this research was conducted at the Center for Nanophase Materials Sciences, which is a DOE Office of Science User Facility. This work was supported by Basic Science Research Program through the National Research Foundation of Korea (NRF) funded by the Ministry of Education (2016R1D1A3B03931932). This work was also supported by a grant (2015M1A2A2056218) from the Technology Development Program to Solve Climate Changes of the NRF funded by MSIP. SMK acknowledges support from the National Science Foundation (Award # 1512221).

Notes and references

1 U. Tritschler, S. Pearce, J. Gwyther, G. R. Whittell and I. Manners, *Macromolecules*, 2017, **50**, 3439-3463.
2 F. H. Schacher, P. A. Rupar and I. Manners, *Angew. Chem. Int. Ed.*, 2012, **51**, 7898-7921.
3 J.-F. Gohy, *Adv. Polym. Sci.* 2005, **190**, 65-136.
4 Y. Mai and A. Eisenberg, *Chem. Soc. Rev.*, 2012, **41**, 5969-5985.
5 B. D. Olsen and R. A. Segalman, *Mater. Sci. Eng. R Rep.*, 2008, **62**, 37-66.
6 K. Bornani, X. Wang, J. L. Davis, X. Wang, W. Wang, J. P. Hinestrosa, J. W. Mays and S. M. Kilbey II, *Soft Matter*, 2015, **11**, 6509-6519.
7 X. Li, P. J. Wolanin, L. R. MacFarlane, R. L. Harniman, J. Qian, O. E. C. Gould, T. G. Dane, J. Rudin, M. J. Cryan, T. Schmaltz, H. Frauenrath, M. A. Winnik, C. F. J. Faul and I. Manners, *Nat. Comm.*, 2017, **8**, 15909.

This journal is © The Royal Society of Chemistry 20xx

8 C. Guo, Y.-H. Lin, M. D. Witman, K. A. Smith, C. Wang, A. Hexemer, J. Strzalka, E. D. Gomez and R. Verduzco, *Nano Lett.*, 2013, **13**, 2957-2963.
9 X. Yu, K. Xiao, J. Chen, N. V. Lavrik, K. Hong, B. G. Sumpter and D. B. Geohegan, *ACS Nano*, 2011, **5**, 3559-3567.
10 J.-Y. Lee, C.-J. Lin, C.-T. Lo, J.-C. Tsai and W.-C. Chen, *Macromolecules*, 2013, **46**, 3005-3014.
11 N. E. Persson, P.-H. Chu, M. McBride, M. Grover and E. Reichmanis, *Acc. Chem. Res.*, 2017, **50**, 932-942.
12 J. A. Lim, F. Liu, S. Ferdous, M. Muthukumar and A. L. Briseno, *Mater. Today*, 2010, **13**, 14-24.
13 S. Agbolaghi and S. Zenoozi, *Org. Electron.*, 2017, **51**, 362-403.
14 X. Pang, C. Feng, H. Xu, W. Han, X. Xin, H. Xia, F. Qiu and Z. Lin, *Polym. Chem*., 2014, **5**, 2747 –2755
15 L. Zhao, C. Feng, X. Pang, J. Jung, M. C. Stefan, P. Sista, R. Han, N. Fang and Z. Lin, *Soft Matter*, 2013, **9**, 8050–8056
16 S. Pan, L. He, J. Peng, F. Qiu and Z. Lin, *Angew. Chem. Int. Ed.* 2016, **55**, 8686–8690
17 M. He, L. Zhao, J. Wang, W. Han, Y. Yang, F. Qiu and Z. Lin, *ACS Nano*, 2010, **4**, 3241-3247.
18 M. H. M. Cativo, D. K. Kim, R. A. Riggleman, K. G. Yager, S. S. Nonnenmann, H. Chao, D. A. Bonnell, C. T. Black, C. R. Kagan and S.-J. Park, *ACS Nano*, 2014, **8**, 12755-12762.
19 J. B. Gilroy, D. J. Lunn, S. K. Patra, G. R. Whittell, M. A. Winnik and I. Manners, *Macromolecules*, 2012, **45**, 5806-5815.
20 S.-J. Park, S.-G. Kang, M. Fryd, J. G. Saven and S.-J. Park, *J. Am. Chem. Soc.*, 2010, **132**, 9931-9933.
21 Z. Li, R. J. Ono, Z.-Q. Wu and C. W. Bielawski, *Chem. Comm.*, 2011, **47**, 197-199.
22 M. Su, S.-Y. Shi, Q. Wang, N. Liu, J. Yin, C. Liu, Y. Ding and Z.-Q. Wu, *Polym. Chem.* 2015, **6**, 6519-6528.
23 I. Y. Song, J. Kim, M. J. Im, B. J. Moon and T. Park, *Macromolecules*, 2012, **45**, 5058-5068.
24 E. Lee, B. Hammer, J.-K. Kim, Z. Page, T. Emrick and R. C. Hayward, *J. Am. Chem. Soc.,* 2011, **133**, 10390-10393.
25 A. C. Kamps, M. H. M. Cativo, M. Fryd and S.-J. Park, *Macromolecules*, 2014, **47**, 161-164.
26 A. C. Kamps, M. Fryd and S.-J. Park, *ACS Nano*, 2012, **6**, 2844-2852.
27 I.-H. Lee and T.-L. Choi, *Polym. Chem.*, 2016, **7**, 7135-7141.
28 G. Polymeropoulos, G. Zapsas, K. Ntetsikas, P. Bilalis, Y. Gnanou and N. Hadjichristidis, *Macromolecules*, 2017, **50**, 1253-1290.
29 T. Lee, J. Oh, J. Jeong, H. Jung, J. Huh, T. Chang and H.-j. Paik, *Macromolecules*, 2016, **49**, 3672-3680.
30 M. Kapnistos, M. Lang, D. Vlassopoulos, W. Pyckhout-Hintzen, D. Richter, D. Cho, T. Chang and M. Rubinstein, *Nat. Mater.*, 2008, **7**, 997.
31 M. M. Hasani-Sadrabadi, V. Karimkhani, F. S. Majedi, J. J. Van Dersarl, E. Dashtimoghadam, F. Afshar-Taromi, H. Mirzadeh, A. Bertsch, K. I. Jacob, P. Renaud, F. J. Stadler and I. Kim, *Adv. Mater.*, 2014, **26**, 3118-3123.
32 A. Mishra, C.-Q. Ma and P. Bäuerle, *Chem. Rev.*, 2009, **109**, 1141-1276.
33 B. C. Popere, A. M. D. Pelle, A. Poe and S. Thayumanavan, *Phys. Chem. Chem. Phys*., 2012, **14**, 4043-4057.
34 M. Scheuble, M. Goll and S. Ludwigs, *Macromol. Rapid Commun.*, 2015, **36**, 115-137.
35 Ž. Tomović, J. van Dongen, S. J. George, H. Xu, W. Pisula, P. Leclère, M. M. J. Smulders, S. De Feyter, E. W. Meijer and A. P. H. J. Schenning, *J. Am. Chem. Soc.*, 2007, **129**, 16190-16196.
36 R. Verduzco, X. Li, S. L. Pesek and G. E. Stein, *Chem. Soc. Rev.*, 2015, **44**, 2405-2420.
37 H.-i. Lee, J. Pietrasik, S. S. Sheiko and K. Matyjaszewski, *Prog. Polym. Sci.*, 2010, **35**, 24-44.
38 J. Rzayev, *ACS Macro Lett.*, 2012, **1**, 1146-1149.
39 M. Müllner and A. H. E. Müller, *Polymer*, 2016, **98**, 389-401.
40 Z. Zhang, J.-M. Y. Carrillo, S.-k. Ahn, B. Wu, K. Hong, G. S. Smith and C. Do, *Macromolecules*, 2014, **47**, 5808-5814.
41 W. Gu, J. Huh, S. W. Hong, B. R. Sveinbjornsson, C. Park, R. H. Grubbs and T. P. Russell, *ACS Nano*, 2013, **7**, 2551-2558.
42 J. Bolton, T. S. Bailey and J. Rzayev, *Nano Lett.*, 2011, **11**, 998-1001.
43 T.-P. Lin, A. B. Chang, S.-X. Luo, H.-Y. Chen, B. Lee and R. H. Grubbs, *ACS Nano*, 2017, **11**, 11632-11641.
44 S. W. Hong, W. Gu, J. Huh, B. R. Sveinbjornsson, G. Jeong, R. H. Grubbs and T. P. Russell, *ACS Nano*, 2013, **7**, 9684-9692.
45 W. Lee, S. Park, Y. Kim, V. Sethuraman, N. Rebello, V. Ganesan and D. Y. Ryu, *Macromolecules*, 2017, **50**, 5858-5866.
46 G. Sun, S. Cho, C. Clark, S. V. Verkhoturov, M. J. Eller, A. Li, A. Pavía-Jiménez, E. A. Schweikert, J. W. Thackeray, P. Trefonas and K. L. Wooley, *J. Am. Chem. Soc.*, 2013, **135**, 4203-4206.
47 R. Fenyves, M. Schmutz, I. J. Horner, F. V. Bright and J. Rzayev, *J. Am. Chem. Soc.*, 2014, **136**, 7762-7770.
48 H. Luo, M. Szymusiak, E. A. Garcia, L. L. Lock, H. Cui, Y. Liu and M. Herrera-Alonso, *Macromolecules*, 2017, **50**, 2201-2206.
49 Z. Li, J. Ma, N. S. Lee and K. L. Wooley, *J. Am. Chem. Soc.*, 2011, **133**, 1228-1231.
50 Y. Gai, D.-P. Song, B. M. Yavitt and J. J. Watkins, *Macromolecules*, 2017, **50**, 1503-1511.
51 X. Li, S. L. Prukop, S. L. Biswal and R. Verduzco, *Macromolecules*, 2012, **45**, 7118-7127.
52 Y. Choo, L. H. Mahajan, M. Gopinadhan, D. Ndaya, P. Deshmukh, R. M. Kasi and C. O. Osuji, *Macromolecules*, 2015, **48**, 8315-8322.
53 P. Deshmukh, S.-k. Ahn, M. Gopinadhan, C. O. Osuji and R. M. Kasi, *Macromolecules*, 2013, **46**, 4558-4566.
54 S.-k. Ahn, J. M. Y. Carrillo, J. Keum, J. Chen, D. Uhrig, b. lokitz, B. G. Sumpter and S. M. Kilbey, *Nanoscale*, 2017, **9**, 7071-7080.
55 Y. Xia, B. D. Olsen, J. A. Kornfield and R. H. Grubbs, *J. Am. Chem. Soc.*, 2009, **131**, 18525-18532.
56 J. A. Love, J. P. Morgan, T. M. Trnka and R. H. Grubbs, *Angew. Chem. Int. Ed.*, 2002, **41**, 4035-4037.
57 S.-k. Ahn, D. L. Pickel, W. M. Kochemba, J. Chen, D. Uhrig, J. P. Hinestrosa, J.-M. Carrillo, M. Shao, C. Do, J. M. Messman, W. M. Brown, B. G. Sumpter and S. M. Kilbey, *ACS Macro Lett.*, 2013, **2**, 761-765.
58 S.-k. Ahn, J.-M. Y. Carrillo, Y. Han, T.-H. Kim, D. Uhrig, D. L. Pickel, K. Hong, S. M. Kilbey, B. G. Sumpter, G. S. Smith and C. Do, *ACS Macro Lett.*, 2014, **3**, 862-866.
59 K. Tremel and S. Ludwigs, *Adv. Polym. Sci.*, 2014, 265, 39-82.
60 R. Colle, G. Grosso, A. Ronzani and C. M. Zicovich-Wilson, *Phys Status Solidi B*, 2011, **248**, 1360-1368.
61 F. Liu, Y. Gu, J. W. Jung, W. H. Jo and T. P. Russell, *J. Polym. Sci. Part B: Polym. Phys.*, 2012, 50, 1018-1044.
62 J. Zhao, A. Swinnen, G. Van Assche, J. Manca, D. Vanderzande and B. V. Mele, *J. Phys. Chem. B*, 2009, **113**, 1587-1591.
63 S. Y. Yu-Su, S. S. Sheiko, H.-i. Lee, W. Jakubowski, A. Nese, K. Matyjaszewski, D. Anokhin and D. A. Ivanov, *Macromolecules,* 2009, **42,** 9008-9017.
64 N. Xia, G. Zhang, T. Li, W. Wang, H. Zhu, Y. Chen and G. Deng, *Polymer*, 2011, **52**, 4581-4589.
65 P. Deshmukh, S.-k. Ahn, L. Geelhand de Merxem and R. M. Kasi, *Macromolecules*, 2013, **46**, 8245-8252.
66 S. Kripotou, C. Psylla, K. Kyriakos, K. N. Raftopoulos, J. Zhao, G. Zhang, S. Pispas, C. M. Papadakis and A. Kyritsis, *Macromolecules,* 2016, **49**, 5963-5977.
67 S. Samitsu, T. Shimomura, S. Heike, T. Hashizume and K. Ito, *Macromolecules*, 2008, **41**, 8000-8010.

68 Y. D. Park, H. S. Lee, Y. J. Choi, D. Kwak, J. H. Cho, S. Lee and K. Cho, *Adv. Funct. Mater.*, 2009, **19**, 1200-1206.
69 J. Alonzo, W. M. Kochemba, D. L. Pickel, M. Ramanathan, Z. Sun, D. Li, J. Chen, B. G. Sumpter, W. T. Heller and S. M. Kilbey II, *Nanoscale*, 2013, **5**, 9357-9364.

This journal is © The Royal Society of Chemistry 20xx

Table of Contents

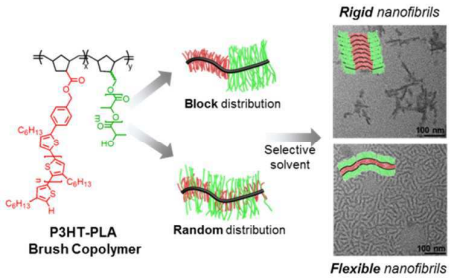

Solution self-assembly of P3HT-containing copolymers was tailored effectively via bottlebrush architecture, particularly by tuning its side chain arrangement as well as copolymer composition.